14.1

Estimation of the size of SARS-CoV-2 viral particles based on Small-angle X-ray scattering data in the application for SERS spectroscopy

© A.T. Tabarov[1], D.A. Krylov[1], O.V. Andreeva[1], A.V. Smirnov[1], D.M. Danilenko[2], V.V. Vitkin[1]

[1] ITMO University, St. Petersburg, Russia
[2] Smorodintsev Research Institute of Influenza (a Russian Ministry of Health federal institution), St. Petersburg, Russia
E-mail: a_t_tabarov@itmo.ru

Received December 18, 2023
Revised February 25, 2024
Accepted February 26, 2024

Using small-angle X-ray scattering (SAXS), the pairwise distance function of SARS-CoV-2 viral particles has been determined. The influence of surface proteins, which create a loosened structure on the virus surface, on the results of viral particle size determination is discussed. The obtained results are of interest for the development of selective SERS substrates for the diagnosis of coronavirus infection.

Keywords: Viruses, small-angle scattering, X-ray, synchrotron studies.

DOI: 10.61011/TPL.2024.06.58469.19848

Classical techniques for diagnostics of viral diseases (SARS-CoV-2), such as PCR testing, turned out to be inefficient in the context of mass infection [1]. New diagnostic methods, of which surface-enhanced Raman spectroscopy (SERS) is an example [2], are being examined at present. Data on the size of viral particles [3], which is hard to measure with an electron microscope (EM), are important for the construction of a selective SERS substrate. Literature data on the sizes of viral particles measured with an EM cover a wide range of values: 60−140 nm [4] or 50−200 nm [5].

In the present study, small-angle X-ray scattering (SAXS) was used to examine a suspension of inactivated viral particles. This technique allows one to estimate their size and other parameters [6,7]. Coronavirus line CL.1 of strain hCoV-19/Russia/PER-RII-MH117274/2022 was used in the study. Following cultivation, solutions of formaldehyde and beta-propiolactone (BPL) were added to the samples with viruses. The following inactivator/suspension ratios were examined: 1:1000, 1:500, and 1:250. Example images of studied viruses obtained with an EM are shown in Fig. 1. The concentration of viral proteins in samples was measured using the Lowry method. Six samples of virus-containing suspensions were examined (see the table).

Experiments were carried out at the BIOSAX beamline of the „KISI-Kurchatov“ source with the use of synchrotron radiation from the „Sibir-2“ accelerator. X-ray patterns were recorded with a DECTRIS Pilatus3 1M two-coordinate detector at a distance of 2500 mm. The sample−detector distance was adjusted accurately with the use of the Fit2D program and silver behenate (as a calibration standard). The scattering intensity was measured within the $0.04 < s < 1.5\,\mathrm{nm}^{-1}$ range, where s is the scattering vector magnitude.

Twelve SAXS curve measurements (each with an exposure of 600 s) were performed for each of the six samples. The PRIMUS program from the ATSAS specialized package [8] was used to process the obtained data, which involved averaging of scattering curves and subtracting the buffer signal. The size of viral particles was determined in two ways: based on the pair distance distribution function ($D_{\max}$) and the radius of gyration (R_g).

Curves were analyzed using the Distance Distribution tool (PRIMUS [9]) in the monodisperse mode. It is implied in this mode that the studied system consists of particles of the same (not necessarily spherical) shape and size. This is a simplifying assumption, since both spherical viruses and pear-shaped detached surface proteins (spike proteins), which are significantly smaller than viruses, are present in the suspension. In the monodisperse mode, the Distance Distribution tool provides an opportunity to determine pair distance distribution function $p(r)$ [6]:

$$p(r) = \frac{r^2}{2\pi^2} \int_0^{D_{\max}} s^2 I(s) \frac{\sin(sr)}{sr}\, ds, \qquad (1)$$

where r is the distance between two particles and $I(s)$ is the experimental scattered radiation intensity.

Function $p(r)$ provides an opportunity to estimate maximum particle size $D_{\max}$ based on the condition that $p(r) = 0$ at $r > D_{\max}$. The sample shape may also be inferred from the form of function $p(r)$. When the plot of function $p(r)$ corresponds to a uniform sphere, its radius is

$$R_D = \frac{D_{\max}}{2}. \qquad (2)$$

Function $p(r)$ was plotted for all samples. A total of 286 points within the $0.04 < s < 0.88\,\mathrm{nm}^{-1}$ range of scattering vector magnitudes were used for each sample.

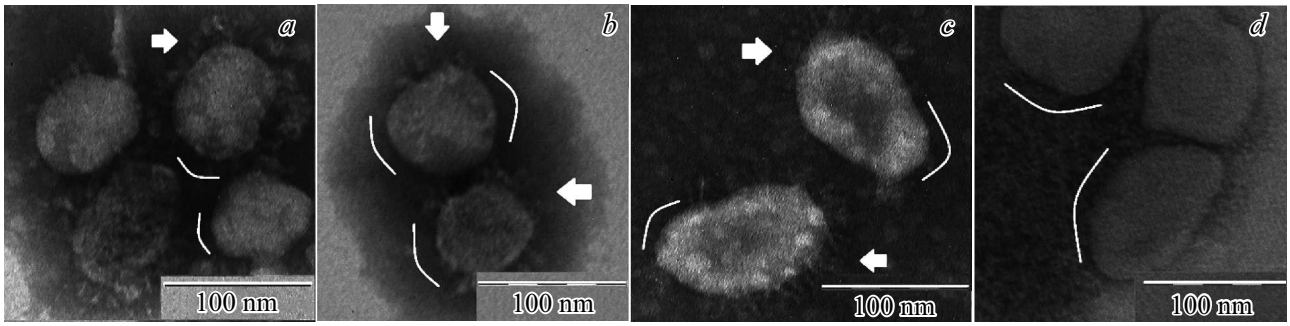

Figure 1. Inactivated viruses imaged with an electron microscope. *a* — Inactivation with formaldehyde, 1:1000; *b* — inactivation with formaldehyde, 1:250; *c* — inactivation with BPL, 1:1000; and *d* — inactivation with BPL, 1:250. Arrows point at the regions where surface proteins were retained. The regions where viruses have lost surface proteins are designated with lines. Formaldehyde partly cross-links surface proteins and partly facilitates their detachment, while BPL has a stronger influence on protein detachment and virus morphology.

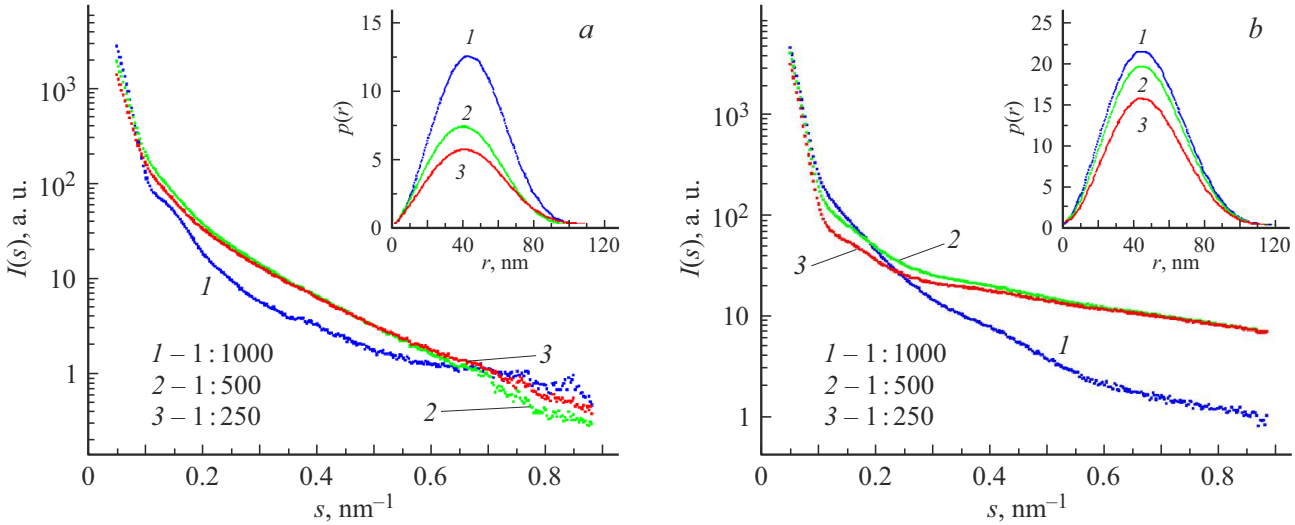

Figure 2. Dependence of the logarithm of intensity of scattered radiation $I(s)$ on the scattering vector magnitude and pair distance distribution functions (insets). *a* — Samples inactivated with formaldehyde; *b* — samples inactivated with BPL. The $0.04 < s < 0.1\,\mathrm{nm}^{-1}$ section of the curve corresponds to scattering off large viral particles, while the contribution of smaller detached proteins is manifested at $0.1 < s < 0.88\,\mathrm{nm}^{-1}$. The intensity of scattering off proteins increases with increasing concentration of the inactivating agent in the sample.

The GNOM utility from the ATSAS package allowed us to determine radius of gyration R_g. Radius R_I of a uniform sphere and its radius of gyration R_g are related in a simple way [6]:

$$R_I = \sqrt{\frac{5}{3}} R_g. \qquad (3)$$

The sizes of viral particles are estimated from pair distance distribution function $p(r)$ (formula (1)) and the radius of gyration (formula (3)).

Having integrated two-dimensional scattering patterns, we obtained scattering curves (Fig. 2) that represent the dependence of scattered radiation intensity $I(s)$ on scattering vector magnitude s. The upward shift of the intensity curve on the right-hand side of the plot, which corresponds to smaller structures, is representative of the increased relative fraction of detached surface proteins in the suspension. Thus, the degree of inactivation of samples affects the scattered radiation intensity. The obtained values of viral particle radii are listed in the table. The average or, in other words, the most probable size (diameter) of a SARS-CoV-2 particle was determined as a result: $112 \pm 5\,\mathrm{nm}$. The obtained data should help fabricate selective SERS substrates with a high amplification factor and enhance the efficiency of COVID-19 diagnostic techniques. The mismatch between radius R_I, which was calculated from radius of gyration R_g, and radius R_D, which was determined from pair distance distribution function $p(r)$, is largely attributable to the presence of proteins that produce a loosened structure on the virus surface. Radius R_I, which was calculated from radius of gyration R_g that is a normalized integral characteristic, is less affected by the presence of surface proteins than

Results of measurement of viral particle radius R_D and R_I based on $D_{\max}$ and R_g

№	Sample	Degree of inactivation	Protein concentration, mg/ml	$D_{\max}$, nm	R_D, nm	R_g, nm	R_I, nm
1	CL.1 Form.	1:1000	1.61	117	58.5	35.9	46.4
2	CL.1 Form.	1:500	1.77	115	57.5	35.9	46.3
3	CL.1 Form.	1:250	1.58	114	57.0	35.8	46.2
4	CL.1 BPL	1:1000	1.8	105	52.5	34.3	44.3
5	CL.1 BPL	1:500	2.24	110	55.0	33.8	43.6
6	CL.1 BPL	1:250	1.97	110	55.0	33.5	43.2
Average value				112 ± 5	56 ± 2	35 ± 1	45 ± 2

Note. Coronavirus strain CL.1 was inactivated with formaldehyde (Form.) and BPL. The inactivator/virus-containing suspension ratio is indicated. The last row contains the average values of radii with the mean-square deviation and the program error taken into account.

R_D, which was determined from pairwise distance function $p(r)$.

Acknowledgments

The authors wish to thank E.V. Shtykova for useful suggestions and remarks.

Funding

This study was supported financially by the Ministry of Science and Higher Education of the Russian Federation (project 075-15-2021-1349).

Conflict of interest

The authors declare that they have no conflict of interest.

References

[1] J.N. Kanji, N. Zelyas, C. MacDonald, K. Pabbaraju, M.N. Khan, A. Prasad, J. Hu, M. Diggle, B.M. Berenger, G. Tipples, Virol. J., **18** (1), 13 (2021). DOI: 10.1186/s12985-021-01489-0

[2] A. Tabarov, V. Vitkin, O. Andreeva, A. Shemanaeva, E. Popov, A. Dobroslavin, V. Kurikova, O. Kuznetsova, K. Grigorenko, I. Tzibizov, A. Kovalev, V. Savchenko, A. Zheltuhina, A. Gorshkov, D. Danilenko, Biosensors, **12** (12), 1065 (2022). DOI: 10.3390/bios12121065

[3] Y.Y. Lin, J.D. Liao, M.L. Yang, C.L. Wu, Biosensors Bioelectron., **35** (1), 447 (2012). DOI: 10.1016/j.bios.2012.02.041

[4] N. Zhu, D. Zhang, W. Wang, X. Li, B. Yang, J. Song, X. Zhao, B. Huang, W. Shi, R. Lu, P. Niu, F. Zhan, X. Ma, D. Wang, W. Xu, G. Wu, G.F. Gao, D. Phil, W. Tan, New Engl. J. Med., **382** (8), 727 (2020). DOI: 10.1056/NEJMoa2001017

[5] D. Kota, Int. J. Collab. Res. Intern. Med. Public Health, **13** (6), 1 (2021). https://www.iomcworld.org/articles/coronavirus-and-its-structure-80809.html

[6] L.A. Feigin, D.I. Svergun, *Structure analysis by small-angle X-ray and neutron scattering* (Plenum Press, N.Y., 1987). DOI: 10.1007/978-1-4757-6624-0.

[7] E.V. Shtykova, M.V. Petukhov, N.V. Fedorova, A.M. Arutunyan, A.M. Skurat, L.V. Kordukova, A.V. Moiseevnko, A.L. Ksenofontov, Biochemistry (Moscow), **86** (2), 230 (2021). DOI: 10.1134/S0006297921020115.

[8] K. Manalastas-Cantos, P.V. Konarev, N.R. Hajizadeh, A.G. Kikhney, M.V. Petoukhov, D.S. Molodenskiy, D. Franke, J. Appl. Cryst., **54** (1), 343 (2021). DOI: 10.1107/S1600576720013412

[9] P.V. Konarev, V.V. Volkov, A.V. Sokolova, M.H. Koch, D.I. Svergun, J. Appl. Cryst., **36** (5), 1277 (2003). DOI: 10.1107/S0021889803012779

Translated by D.Safin